Virtual incidence effect on rotating airfoils in Darrieus wind turbines

Publisher's version at DOI: 10.1016/j.enconman.2015.12.056

Virtual incidence effect on rotating airfoils in Darrieus wind turbines

Alessandro Bianchini[1a], Francesco Balduzzi[1b], Giovanni Ferrara[1c], Lorenzo Ferrari[2d]

[1)] Department of Industrial Engineering, University of Florence
Via di Santa Marta 3, 50139, Florence, Italy
Phone +39 055 275 8773

[3)] CNR-ICCOM, National Research Council of Italy
Via Madonna del Piano 10, 50019, Sesto Fiorentino, Italy
Phone +39 055 5225 218 - Fax +39 055 5225 203

Abstract

Small Darrieus wind turbines are one of the most interesting emerging technologies in the renewable energies scenario, even if they still are characterized by lower efficiencies than those of conventional horizontal-axis wind turbines due to the more complex aerodynamics involved in their functioning. In case of small rotors, in which the chord-to-radius ratios are generally high not to limit the blade Reynolds number, the performance of turbine blades has been suggested to be moreover influenced by the so-called "flow curvature effects". Recent works have indeed shown that the curved flowpath encountered by the blades makes them work like virtually cambered airfoils in a rectilinear flow.

In the present study, focus is instead given to a further effect that is generated in reason of the curved streamline incoming on the blades, i.e. an extra-incidence seen by the airfoil, generally referred to as "virtual incidence". In detail, a novel computational method to define the incidence angle has been applied to unsteady CFD simulations of three airfoils in a Darrieus-like motion and their effective angles of attack have been compared to theoretical expectations.

The analysis confirmed the presence of an additional virtual incidence on the airfoils and quantified it for different airfoils, chord-to-radius ratios and tip-speed ratios. A comparative discussion on BEM prediction capabilities is finally reported in the study.

Keywords: Darrieus, vertical axis wind turbine, flow curvature, virtual incidence, CFD, angle of attack, BEM

1. Introduction

Increasing interest is presently being paid to understand where, beyond large wind farms, small and medium-size wind turbines can represent an alternative for delocalized power production [1], with particular focus on off-grid applications (e.g. [2-3]). *Inter alia*, the built and populated environment presently represent the research frontier [4], since the produced power could be immediately available for a large number of applications or simply used to reduce the energy demand of buildings [5]. Even in the flows in this environment are generally very complex, if properly positioned small turbines are thought to take advantage from augmented wind speeds [6] or specific interactions with the buildings [7].

a) bianchini@vega.de.unifi.it *b) balduzzi@vega.de.unifi.it*
c) giovanni.ferrara@unifi.it *d) lorenzo.ferrari@iccom.cnr.it (*=corresponding author)*

Among other technologies, Vertical-Axis Wind Turbines (VAWTs), both drag (e.g. [8-9]) and lift-driven (e.g. [10-11]), are gaining popularity in view of similar applications, since they can work effectively even in presence of low-speed and unstructured flows with low noise emissions and high reliability [12]. In particular, Darrieus rotors are increasingly appreciated, as they are probably the only ones able to reach efficiencies somehow competitive with respect to Horizontal-Axis Wind Turbines (HAWTs) [13]. Moreover, differently from HAWTs, they are supposed to even improve their power coefficient in case of skewed flow [14-15].

At the present state-of-the-art, however, the global efficiencies of Darrieus turbines still lack from those of HAWTs, due to their intrinsically more complex aerodynamics coming from the revolution of blades around an axis orthogonal to flow direction. This generates a continuous variation of the angle of attack, which leads to additional phenomena, like for example dynamic stall [13].

Recently, a study by Bianchini et al. [16] demonstrated that the so-called “flow curvature effects” represent one of the main aspects to be assessed in order to achieve a deeper understanding of Darrieus turbines’ aerodynamics. The first studies on these phenomena date back to the early ‘90s, when Migliore et al. [17], based on a one-dimensional analysis of the attended velocity vectors along the airfoil, theorized that the curved path VAWT blades follow imparts a *virtual camber* and a *virtual incidence* on them, i.e. that their performance would be analogous to that of a cambered blade at modified incidence in a rectilinear flow (see Fig. 1). Migliore and his colleagues anyhow theorized these effects only using non-dimensional theories and did not verified it on real turbines.

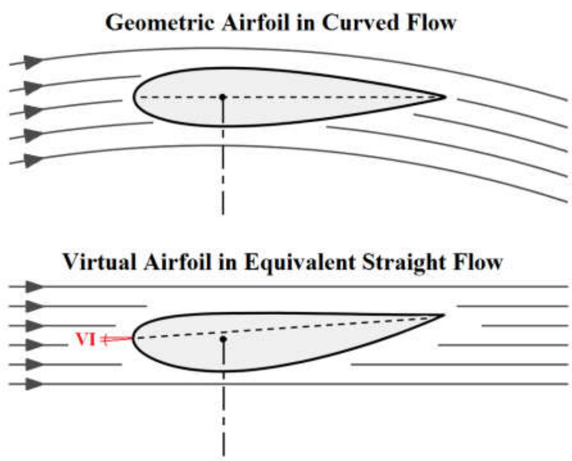

Figure 1 - Flow curvature effects on an airfoil in Darrieus-like motion.

A recent work published by the authors have shown that the associated differences in performance between “geometrical” and “virtual” airfoils become a source of error in any analysis using the original blade profile’s data [18]. Their attention was however fully focused on the virtual camber effect.

This study sets out instead to both assess the presence of the virtual incidence and to estimate its impact on airfoil’s performance in order to judge how best account for it in low-order simulation methods, like Blade Element Momentum (BEM) codes.

To do so, the same three airfoils analyzed in Ref. [18] were considered, i.e. a conventional symmetric NACA 0018 and two modified profiles based on it. In details, the two modified profiles have been conformally transformed to fit their camber lines to the arc of a circle, such that the ratio between the airfoil chord and the circle’s radius, c/R, is 0.114 or 0.25 (Fig. 2).

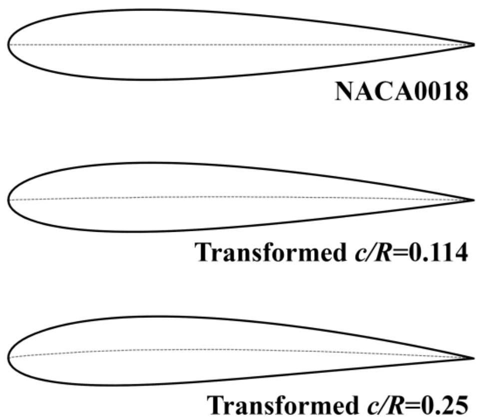

Figure 2 – The three profiles used in this study.

The two *c/*R values were selected as compatible with the ones originally used by Migliore [17], whose theory was used as a comparison in the present study. Based on the applied transformations, the c/R = 0.114 airfoil has a maximum camber of 1.42% at 50% of chord, while the c/R = 0.25 has 3.11% maximum camber, again at 50% of chord. Following the indications of Ref. [18], it has to be attended that "in tunnel-like flow condition the transformed airfoils should perform as the unmodified NACA 0018 would in VAWTs with similar c/R ratios and conversely the NACA 0018's results in rectilinear flow should correspond to those of the transformed airfoils when used in the VAWTs" [18].

To analyze the airfoil's behavior and then estimate the actual incidence they are experiencing, CFD simulations have been carried out at different tip-speed ratios and analyzed in terms of incidence angles experienced by the profiles using a novel method developed by the authors [19].

2. Case study and CFD simulations

CFD simulations were used to investigate the aerodynamic behavior of the selected airfoils when rotating onboard a Darrieus turbine. The use of CFD to go into the aerodynamics details of the phenomena and then define proper corrections to be transferred to low-order simulation methods is indeed a recent trend in the research, which is disclosing very interesting horizons for a further comprehension of many details of airfoils' functioning (e.g. [20-21]).

Four "single-bladed" rotors were considered, obtained by combining the two c/R ratios with both the NACA 0018 and the relevant transformed airfoils in each case.

Table 1 reports the main geometrical features of the four simulated models. The airfoil chord was kept constant in all the simulations, while the revolution radius was changed to achieve the two desired chord-to-radius ratios.

Table 1 – Test cases.

	Case 1	**Case 2**	**Case 3**	**Case 4**
c/R	0.114		0.25	
airfoil	NACA0018	Transformed (c/R=0.114)	NACA0018	Transformed (c/R=0.25)
c [m]	0.20	0.20	0.20	0.20
R [m]	1.75	1.75	0.80	0.80
U [m/s]	8.0	8.0	8.0	8.0

The authors have presented in recent works [22-23] the assessment and validation of the main numerical settings that have been used in CFD simulations. The validity of these settings has been verified by comparing simulations to several experimental data, both in terms of power coefficient vs. tip-speed ratio and of torque profile during the revolution [20], obtaining a constant and very satisfactorily agreement. For completeness, the main settings are anyhow briefly summarized here.

The commercial code ANSYS Fluent [24] was used for the 2D simulations, which made use of a time-dependent unsteady Reynolds-averaged Navier-Stokes (U-RANS) approach, in the pressure based formulation. The Coupled algorithm was employed to handle the pressure-velocity coupling. A dedicated sensitivity analysis [22] and recent studies from the literature [25] indeed showed that this algorithm ensured more robust results when adopting different meshes, timesteps, or rotating speeds. The second order upwind scheme was used for the spatial discretization of the whole set of RANS and turbulence equations, as well as the bounded second order for time differencing to obtain a good resolution [22].

Air was modeled as an ideal compressible gas with standard ambient conditions, i.e. a pressure of 1.01×10^5 Pa and a temperature of 300 K.

The global convergence of each simulation was monitored by considering the difference between the mean values of the torque coefficient over two subsequent revolutions normalized by the mean value over the second period of the pair. The periodicity error threshold was set to 0.1% [22].

Exploiting the sliding-mesh model of the solver, the simulation domain was divided into two subdomains in order to allow the rotation of the turbine, as proposed by Maître et al. [26] and Raciti Castelli et al. [27]. Fig. 3 shows a circular zone containing the turbine, with a diameter (2D) twice that the turbine itself (D). R represents the turbine radius. The circular zone rotates with the angular velocity of the rotor while a rectangular fixed outer zone determines the overall domain extent.

The final dimensions of both domains (reported in Fig.3) were defined according to the sensitivity analysis reported in [22] in order to allow a full development of the turbine wake.

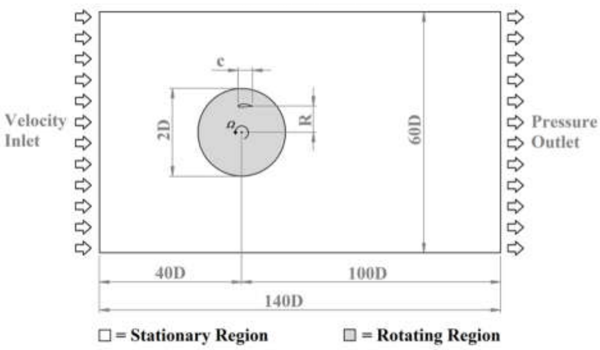

Figure 3 – Simulation domain.

The mesh settings were defined accordingly to the results of the grid-independency analysis reported in [22], where six different levels of refinement of the mesh were tested. An unstructured mesh composed by triangular elements was used for the discretization of the core flow region, whereas the entire boundary layer region has been described with a structured O-grid of 50 layers.

Based on the requirements of the selected turbulence model, the first cell height was selected as to provide a dimensionless wall distance (y^+) during the rotor revolution constantly lower than 1.

The expansion ratio for the growth of elements starting from the surface was kept below 1.1 to achieve good mesh quality in proximity of the airfoil.

Based on [22], the airfoil was discretized with approximately 600 nodes. As a result, the mesh size of the rotating region, for the single-bladed configuration, results in approximately 1.4×10^5 elements, while the stationary region is discretized with 2.0×10^5 elements. Figures 4 and 5 show some details of the grids. The mesh is refined in the region surrounding the blade due to the higher complexity of the flow field. As suggested by [27] and recently demonstrated by [28], a *control circle* (Fig. 4a), with a diameter equal to twice the airfoil's chord, was defined around the blade in order to have a better capability to control the elements size in the region closer to the blade itself.

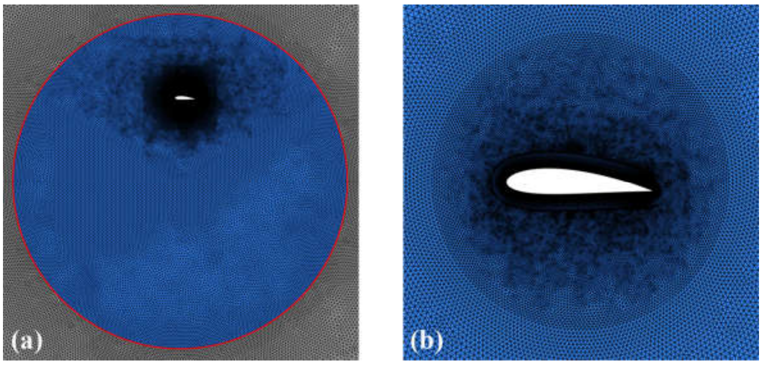

Figure 4 – Computational grid for the rotating domain (a) and control circle details (b) for transformed airfoil with *c/R*=0.25.

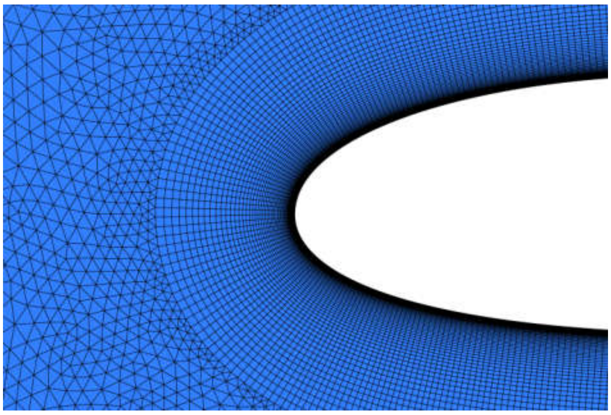

Figure 5 – Computational grid: boundary layer discretization at the leading edge (e.g. transformed airfoil with *c/R*=0.25).

Recent work [22] demonstrated that, in case of Darrieus VAWTs, different functioning TSRs require specific minimum timesteps of CFD simulations in order to ensure accurate results throughout the entire power curve. According to [22], in the present analysis angular timesteps in the range between 0.135° and 0.42° were used, corresponding to the cases with the lowest and the highest TSR respectively.

Concerning the turbulence closure problem, Balduzzi et al. [23], showed the effectiveness of Menter's shear stress transport (*SST*) [29] model in performance simulations involving unsteady aerodynamics for VAWTs, as also confirmed by wide use in literature. In the present study, however, attention has been focused on a more detailed examination of the aerodynamic behavior of each single airfoil in motion by analyzing equivalent static pressure coefficients on the blade profiles. Since the prediction of the boundary layer evolution becomes a critical issue and the blade Reynolds number for the considered cases cannot guarantee a fully turbulent condition, the γ-Re_θ transition model (derived by Menter and Langtry from the SST model [30]) was implemented, despite its increased computational cost. Lanzafame et al. recently showed good agreement between experimental data and numerical results obtained with the transition turbulence model for two different types of H-Darrieus turbines [31].

3. Data analysis

The main concern of the present study is to assess and quantify the virtual incidence (*VI*) seen by the airfoils in motion onboard Darrieus wind turbines.

According to the original work by Migliore, the virtual incidence is defined in Fig. 6 as the difference between the angle of attack really experienced by the airfoil α_P (i.e. that matching the airfoil's performance in straight flow) and the flow angle (i.e. the angle between the relative velocity and the airfoil's chord) in the same point α_F (Eq.1). The angle ψ represents the hypothetical pitch angle between the chord and the tangential direction.

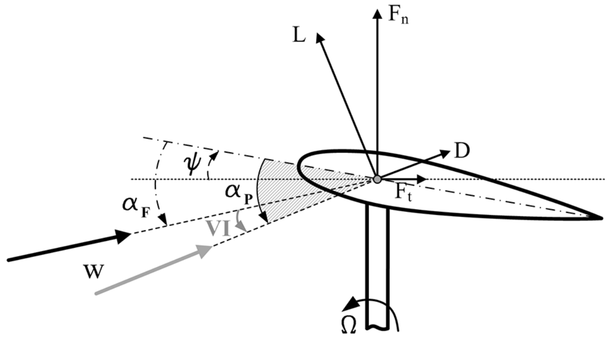

Figure 6 – Definitions and graphical convention.

$$\alpha_P = \alpha_F + VI \qquad (1)$$

In the first estimation by Migliore [17], the flow angle was simply calculated by resolving the velocity triangle composed by the peripheral speed and the undisturbed wind velocity (no induction factor was even provided). On the other hand, the incidence "seen" by the airfoil was estimated accounting for the local angle between the flow direction and the airfoil's surface along the chord.

In the present study, both components have been estimated from CFD with two novel approaches, in order to achieve a much higher degree of confidence on the results and then on the estimation of the virtual camber. To do so, once each simulation had reached full convergence, the pressure distribution over the airfoil and the flow field in proximity of the blades were acquired approximately every 1.5 degrees of azimuthal increment [32].

3.1 Definition of the angle of attack (AoA) and relative speed modulus

In order to investigate the virtual incidence acting on the airfoils, a robust procedure to extrapolate the angle of attack was first needed. This is not an automatic procedure as the concept of incidence angle actually belongs to one-dimensional aerodynamics and cannot be directly transferred to a real flow.

The concern of defining the angle of attack from CFD simulations of rotating blades has been originally addressed by wind turbine specialists in case of HAWTs [33]. In case of Darrieus VAWTs, where the AoA changes constantly during the revolution and the streamline are deflected due to curvature, the definition of an incidence angle is even more complex. Recently, the authors have proposed a novel methodology to extrapolate the AoA from 2D CFD simulations of a Darrieus turbine [19] and have successfully applied it to the study of the virtual camber effect [18], which is part of the method itself.

The same approach has been applied also in the present study and it is briefly summarized below for completeness to the reader. It is a four-steps process [19]:

1. Based on the chord-to-radius ratio of the rotor and the tip-speed ratio, the virtual airfoil due to flow-curvature effects is defined based on the conformal transformations of Migliore et al. [17].
2. The virtual airfoil shape is simulated with a code based on panel methods (e.g. XFoil [34]), obtaining the pressure coefficient distributions for a wide range of AoAs and a Reynolds number compatible with that attended on the airfoil. All the pressure coefficient distributions are then normalized within -1 and +1 by scaling them by their maximum and minimum values. By doing so, the pressure distributions can be compared only based on the incidence angle (by analyzing the position of the pressure peaks [19]), with a negligible error on the exact relative speed, which can be hard to define accurately from CFD calculations.

3. The pressure coefficient distributions are acquired from CFD calculations at different azimuthal positions and again normalized within -1 and +1 by scaling them by their maximum and minimum values.
4. For every azimuthal position, the pressure coefficient distribution from CFD is compared to all those calculated for the airfoils. By doing so, the distributions that best fit together can be highlighted. As discussed, the position along the chord of the pressure peak is mainly used to define the incidence. This comparison directly provides the estimation of the incidence on the airfoil. Moreover, by re-scaling the selected pressure profile to match the dimensional one, the relative speed can be evaluated *a posteriori*.

3.2 Definition of the relative speed direction on the airfoil

If the modulus of relative speed can be obtained following the procedure described above, i.e. counter-scaling the pressure profile in order to match the intensity of pressure gradients on the airfoil, no information is given on the direction of the oncoming wind.

Low-order models (e.g. BEM models) estimate the relative speed by assuming a simple reduction of the modulus of undisturbed wind [35], with no modification of its direction (Eq. 2).

$$\vec{W} = \vec{\omega}R + \vec{U}(1-a) \tag{2}$$

Several experiments (e.g. [36]) and CFD demonstrate, however, that the energy extraction occurring due to the blade-flow interaction contemporarily induces different slowing down and deviation of the flow streamlines approaching a Darrieus rotor, making this approach intrinsically affected by errors. As an example, in Fig. 7a the calculated velocity-field around the transformed airfoil with c/R=0.25 rotating @ TSR=3.1 is reported in terms of modulus and streamlines of the absolute velocity (U).

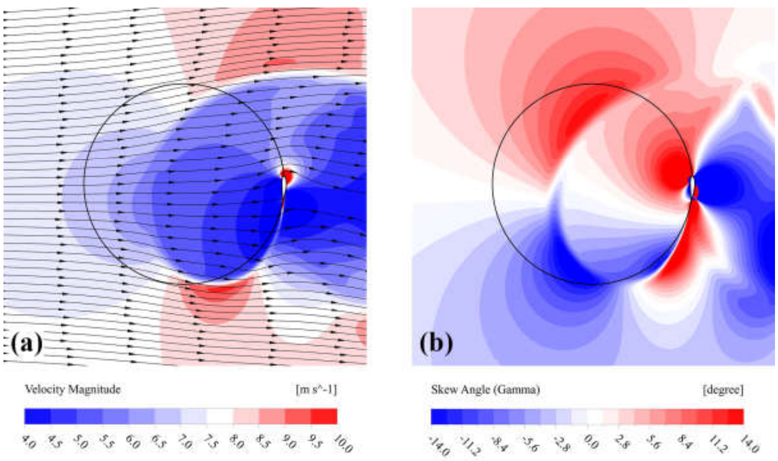

Figure 7 – Transformed airfoil with c/R=0.25 @ TSR=3.3, ϑ=270°: (a) Modulus of the absolute wind speed and streamlines; (b) Skew angle γ.

Upon examination of the figure, it is apparent that the flow is strongly modified when approaching the blade orbit, even if a single rotating airfoil is present (i.e. the rotor has a very low solidity). The undisturbed wind at 8 m/s (neutral color in the figure) cannot reach the airfoil in any point of the revolution. A remarkable drop in the velocity can be instead noticed, together with a deflection of the streamlines.

To overcome the BEM limitation of simply assuming a reduction of the absolute wind velocity, a novel approach was here defined.

Based on the generic velocity triangle of Fig. 8, it is indeed apparent that the peripheral speed is a priori known, both in modulus and direction. Moreover, as discussed before, the modulus of the relative speed can be properly estimated based on the analysis of the pressure coefficient distribution on the airfoil. To completely define the velocity triangle, at least the direction of the absolute wind speed must be then given.

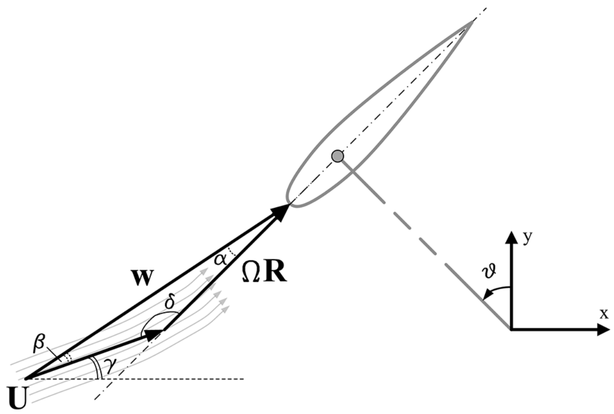

Figure 8 – Definition of the relative speed on the airfoil.

The best estimation of the skew angle γ can be obtained by the computed flow field considering an azimuthal position in which the local flow on the blade only slightly affects the streamlines curvature. By doing so, the deflection of the absolute speed can be estimated to be that induced globally by the energy extraction taking place within the entire rotor.

As an example, in Fig. 7b, the same flow field of Fig. 7a is described in terms of local skew angle of the absolute wind speed. As one may notice, the solidity of the rotor makes it work somehow like a porous media, with a specular deflection of the streamlines with respect to the central one, connecting the azimuthal positions of 90° and 270°.

With the proposed approach, the velocity triangle on the blades can be then fully described, allowing the detailed analysis of the flow around the airfoils with the conventional lumped parameters approach typical of 1D aerodynamics.

3.3 Limitations of the approach

As discussed in literature [32], the validity of the approach for the determination of the effective AoA on the airfoils unfortunately ceases as soon as the flow is separated around the turbine blades. In these conditions, no reliable blade pressure distribution can be obtained with XFoil and therefore no comparison can be made from CFD to XFoil to define the flow incidence on the airfoil itself. Transposing this limitation into an azimuthal range, depending of the airfoil and the TSR, this makes the method working approximately between ϑ=-10° and ϑ=+50°. Beyond this range, the high angles of attack makes the airfoils work in stalled conditions. Moreover, around ϑ=180°, where theoretical AoAs are again reduced, the interaction with the macro-vortices detached around ϑ=90° actually makes the airfoils not experiencing attached flow anymore.

Focusing on the estimation of the skew angle of the wind velocity, limitations are here imposed by the assumption that the airfoil is sufficiently far from the considered azimuthal position not to alter the analyzed flow field. In addition, the presence of macro-vortices makes the local determination of γ nearly impossible in a large portion of the blades motion. Again, the most accurate estimations can be made approximately between ϑ=-10° and ϑ=+60°, then within the same range available for the AoA calculation.

Lastly, the entire approach is soundly more accurate in case of a single rotating blade, in which the interaction of other blades does not affect the oncoming flow on the blade itself. However, once the physics of the phenomena have been assessed, the results can be transposed to any Darrieus turbine of arbitrary solidity.

4. Results and discussion

Fig. 9 reports the calculated virtual incidence *VI* for all the considered airfoils and TSRs as a function of the azimuthal angle of the blade. Results are also compared to the theoretical expectations by Migliore in the same conditions.

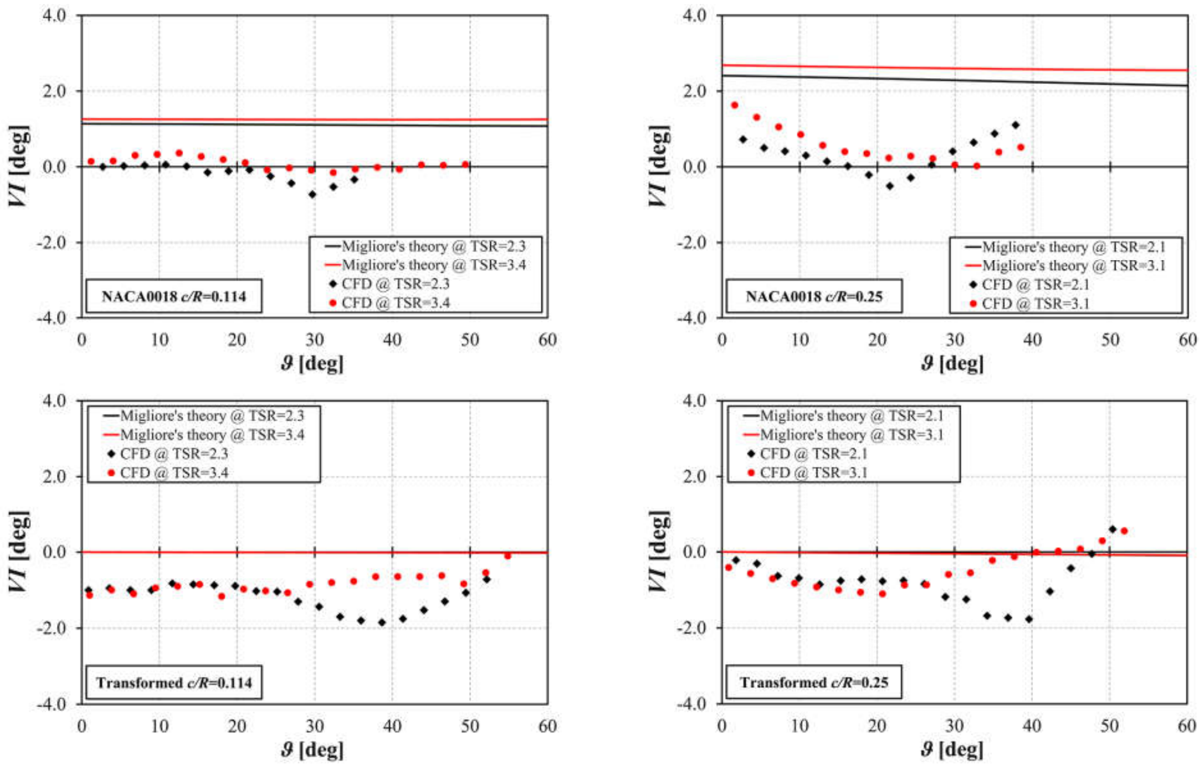

Figure 9 – Virtual Incidence (*VI*) as a function of the azimuthal position of the blade for all the tested configurations compared to Migliore's theoretical expectations.

Upon examination of the figure, some relevant markups can be done:

- Calculated *VI* has the same physical trend than theoretical estimations, being constantly higher for the NACA0018 airfoil than the transformed ones. Moreover, the virtual incidence increases as the chord-to-radius ratio increases. At a fixed *c/R*, it also slightly increases with the TSR, with an anticipated rise towards high AoAs. The influence of the turbine's parameter (*c/R* and TSR) are evident especially for the NACA0018 profiles. On the contrary, the transformed profiles are less sensitive to these parameters since the thickness distribution is symmetric with respect to the blade trajectory, which has the same curvature of the camber line.
- With respect the purely theoretical study of Migliore, calculated values are constantly 1°÷2° lower in modulus. This evidence can be probably related to the fact that Migliore did not assume any induction factor (i.e. slow down) of the wind speed, which is instead experienced in reality due to the energy extraction connected to aerodynamic blade-flow interaction. Moreover, the calculated trends are less smooth since the error in the computation of *VI* values depends on the accuracy of the estimation of various quantities (e.g. α_P, W and γ), which can be easily altered.
- Absolute values appear quite small, but in reality their influence is thought to be absolutely non negligible, as discussed for example in Ref. [35]. In general, where no reliable information of the full azimuthal trend is given, a mean value for *VI* is supposed to anyhow improve the accuracy of theoretical estimations [16].

In order to compare the physical behavior of the airfoils, however, the trend vs. the azimuthal angle is not appropriate as actually referring to different turbine dimensions. To more directly focus on the airfoils, in Fig. 10 and Fig. 11 the trends of *VI* vs. the incidence angles experienced by the airfoils themselves are reported for the NACA0018 and the transformed profiles, respectively.

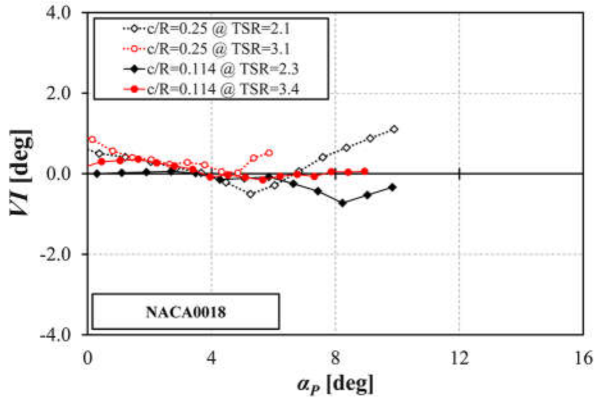

Figure 10 – Virtual Incidence (*VI*) as a function of the AoA for the NACA0018 airfoils in all tested configurations.

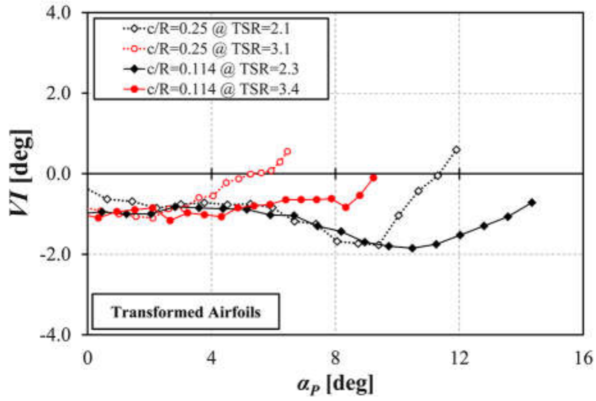

Figure 11 – Virtual Incidence (*VI*) as a function of the AoA for the transformed airfoils in all tested configurations.

Upon examination of the figures, it is apparent that sound agreement was found between the aerodynamic behavior of the two airfoils families. Moreover, it is worth remarking that the *VI* trends are almost identical for the corresponding chord-to-radius ratios for both airfoils, whereas it is confirmed that also the TSR has an influence on the trend as the same angle of attack is reached with a different combination of velocity vectors. For both airfoils, the lowest negative peak of *VI* is obtained at both lower TSR and *c/R* values when the profile experience the largest AoAs. On the other hand, for the smallest AoAs the values are almost identical.

Another set of relevant outcomes is then related to the predicted trend of AoAs as a function of the turbine rotation. This information is indeed of capital relevance to understand if and how BEM codes can be predictive of the real performance of a rotor (provided that the proper aerodynamic coefficients are selected [32]).

Figure 12 reports the calculated AoA trends for all the tested configurations. In the graphs, CFD data are compared to the theoretical expectations of Migliore and to those obtained with a modern BEM code, i.e. the *VARDAR* code of the Department of Industrial Engineering of the University of Florence. In detail, the VARDAR code has been specifically developed for H-Darrieus wind turbines using an improved version of a *Double Multiple Streamtubes Approach with Variable Interference Factors* [13]. The Glauert's correction for the BEM theory has been taken into account with the most recent improvements, together with the corrections due to blades finite Aspect Ratio, using the Lanchester-Prandtl model. In order to increase the accuracy of the aerodynamic estimations, a specific sub model to account for the dynamic stall has been provided, following the Paraschivoiu's adaptation to the DMS approach described in; at the same time, the stream tube expansion along the flow path was considered. For additional details on the code please refer to Refs. [11,37]. The prediction capabilities of the VARDAR code have been validated during a several-years' experience in the design of real H-Darrieus rotors, constantly obtaining good agreement between simulations and experiments.

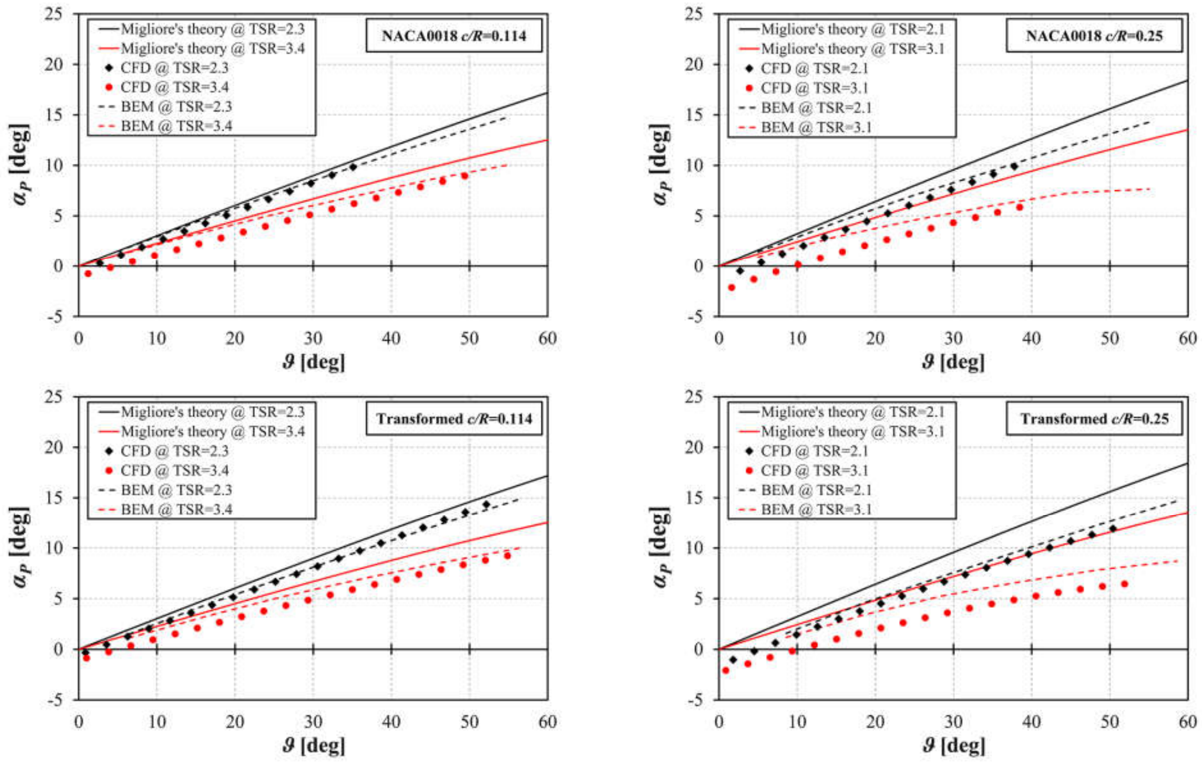

Figure 12 – AoA as a function of the azimuthal position of the blade for all the tested configurations compared to Migliore's theoretical expectations and BEM simulations.

Results are again very interesting. In detail, all the configurations confirmed that:

- Migliore's estimations made without accounting for an induction factor poorly predict the AoAs calculated with CFD, with a spread overestimation of the absolute values and a steeper increase trend.
- The BEM code, even if using the simplified assumption of Eq. 2, predicted quite accurately the AoA trends.
- As attended [18], the BEM predictions are as accurate as the chord-to-radius ratio is low and then the flow curvature effects are reduced. In particular, it is apparent that in all c/R=0.25 configurations BEM simulations still overestimated the AoA at any azimuthal position.

To more clearly understand this behavior, Figure 13 finally reports the skew angle γ of the absolute wind speed as a function of the azimuthal angle for all of the analyzed configurations.

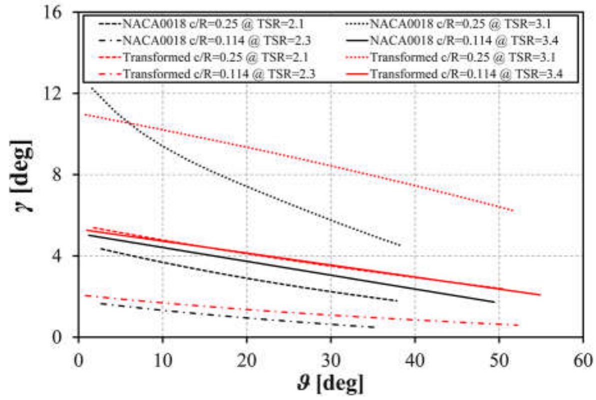

Figure 13 – Skew angle *γ* as a function of the azimuthal angle for the transformed airfoils in all tested configurations.

Figure 13 clearly highlights that in the configurations at high *c/R* ratio, where BEM predictions are poorer, the oncoming wind is more strongly deflected due to the virtual porosity of the rotor. In these conditions, the assumption of only a modulus reduction of the wind velocity leads to a bigger error in the AoA estimations and then on the performance prediction. This is probably one of the main reasons of poorer accuracy of BEM codes for high-solidity turbines [13]. As a visual confirmation, Fig. 14 reports the comparison of the contour plots of the calculated skew angles for the transformed airfoils in the same azimuthal position with *c/R*=0.114 and *c/R*=0.25, respectively. Once again, it is readily noticeable that the more solid turbine imposes a stronger deflection to the oncoming flow, with very high *γ* angles, especially around *ϑ*=0° and *ϑ*=180°.

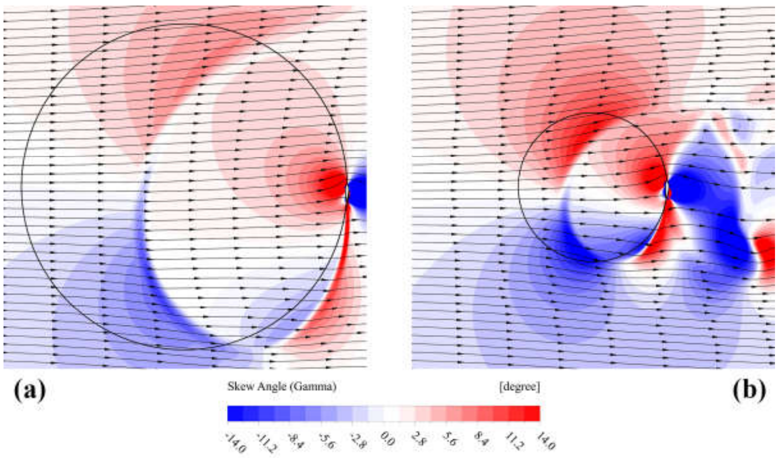

Figure 14 – Calculated skew angles for the transformed airfoils in the same azimuthal position with: (a) *c/R*=0.114; (b) *c/R*=0.25.

5. Conclusions

In the present study, CFD simulations were carried out on a NACA0018 and two airfoils generated by the NACA0018 as to compensate the virtual camber expected in VAWTs with *c/R* = 0.114 and 0.25.

Numerical results were then analyzed with two novel numerical approaches, which provided proper estimations for the angle of attack on the airfoils and the relative speed in modulus and direction.

These data were then used to calculate the Virtual Incidence imparted on the blades due to their motion in a curvilinear flow, i.e. the difference between the angle of attack really experienced by the airfoil and the flow angle (the angle between the relative velocity and the airfoil's chord) in the same point.

Results confirmed that the blades indeed experience a virtual variation in the AoA with respect to theoretical expectations based on the surrounding flow field. In the azimuthal angles range were the proposed approach is applicable, CFD results agreed with the general trends of the original theory even if the absolute values were found to be generally 1°÷2° lower than theoretical ones. In particular, it was proved that: 1) *VI* values were higher for the NACA0018 airfoil than the transformed ones; 2) the virtual incidence increases as the chord-to-radius ratio increases; 3) at a fixed *c/R*, *VI* also slightly increases with the TSR.

In addition, the analysis demonstrated that the wind flow oncoming on a Darrieus rotor is in general strongly deflected by the turbine, with more pronounced values as far as the solidity increases. Notwithstanding this, it was shown that low-order methods, like BEM codes, actually provide quite reliable estimations of the local AoA even if obtained by the incorrect assumption of a simple reduction of the wind velocity modulus.

Finally, it is worth remarking that the presented results are of remarkable interest for a further development of BEM codes. If previous works demonstrated that, in case of high chord-to-radius ratios, the airfoils coefficients of virtually transformed airfoils must be considered in the simulations, it was here proved that further correction should be provided to account for the virtual incidence in order to properly match the real performance of the airfoils.

Acknowledgments

We would like to thank Prof. Ennio Antonio Carnevale of the University of Florence for supporting this research program.

Nomenclature

Acronyms

AoA	Angle of Attack
BEM	Blade Element Momentum
CFD	Computational Fluid Dynamics
HAWTs	Horizontal Axis Wind Turbines
SST	Shear Stress Transport
TSR	Tip-Speed Ratio
U-RANS	Unsteady Reynolds-Averaged Navier-Stokes
VAWTs	Vertical Axis Wind Turbines

Greek symbols

α	Angle of Attack (symbol)	[deg]
β	Angle Between the Wind Speed and the Relative Speed	[deg]
γ	Skew Angle of the Wind Velocity	[deg]
δ	Angle Between the Wind Speed and the Peripheral Speed	[deg]
ϑ	Azimuthal Angle	[deg]
ω	Specific Turbulence Dissipation Rate	[1/s]
Ω	Revolution Speed	[m/s]

Latin symbols

A	Turbine's Swept Area	[m^2]
c	Blade Chord	[m]
D	Rotor Diameter	[m]
k	Turbulence Kinetic Energy	[m^2/s^2]

R	Rotor Radius	[m]
Re_θ	Momentum Thickness Reynolds Number	[-]
U	Undisturbed Wind Speed	[m/s]
VI	Virtual Incidence	[deg]
w	Relative Speed	[m/s]
y^+	Dimensionless Wall Distance	[-]

References

[1] Kirke BK, Evaluation of self-starting vertical axis wind turbines for standalone applications. Ph.D. thesis, Griffith University, Gold Coast (Australia); 1998.

[2] Levent Bilir, Mehmet İmir, Yılser Devrim, Ayhan Albostan, An investigation on wind energy potential and small scale wind turbine performance at İncek region – Ankara, Turkey, Energy Conversion and Management, Volume 103, October 2015, Pages 910-923, ISSN 0196-8904, http://dx.doi.org/10.1016/j.enconman.2015.07.017.

[3] Luai M. Al-Hadhrami, Performance evaluation of small wind turbines for off grid applications in Saudi Arabia, Energy Conversion and Management, Volume 81, May 2014, Pages 19-29, ISSN 0196-8904, http://dx.doi.org/10.1016/j.enconman.2014.01.064.

[4] Mertens S. Wind Energy in the Built Environment. Brentwood (UK): Multi-Science; 2006.

[5] Syngellakis K. Urban wind turbines: Development of the UK market. Proc. of the European Wind Energy Conference 2006, February 27-March 2, Athens (Greece); 2006

[6] Balduzzi F, Bianchini A, Ferrari L. Microeolic turbines in the built environment: influence of the installation site on the potential energy yield. Renewable Energy 2012;45:163-174. DOI**:** 10.1016/j.renene.2012.02.022

[7] Balduzzi F, Bianchini A, Carnevale EA, Ferrari L, Magnani S. Feasibility analysis of a Darrieus vertical-axis wind turbine installation in the rooftop of a building. Applied Energy 2012;97:921–929. DOI: 10.1016/j.apenergy.2011.12.008

[8] Altan BD, Atılgan M, An experimental and numerical study on the improvement of the performance of Savonius wind rotor. Energy Conversion and Management 2008;49(12):3425-3432. DOI: 10.1016/j.enconman.2008.08.021

[9] Bhuyan S, Biswas A. Investigation on self-starting and performance characteristics of simple h and hybrid H-Savonius vertical axis wind rotors. Energy Conversion and Management 2014;87:859-867. DOI: 10.1016/j.enconman.2014.07.056

[10] Willy Tjiu, Tjukup Marnoto, Sohif Mat, Mohd Hafidz Ruslan, Kamaruzzaman Sopian, Darrieus vertical axis wind turbine for power generation I: Assessment of Darrieus VAWT configurations, Renewable Energy, Volume 75, March 2015, Pages 50-67, ISSN 0960-1481, http://dx.doi.org/10.1016/j.renene.2014.09.038.

[11] Bianchini A, Ferrara G, Ferrari L, Design guidelines for H-Darrieus wind turbines: Optimization of the annual energy yield. Energy Conversion and Management 2015;89:690-707. DOI: 10.1016/j.enconman.2014.10.038

[12] Aslam Bhutta MM, Hayat N, Farooq AU, Ali Z, Jamil ShR, Hussain Z, Vertical axis wind turbine – A review of various configurations and design techniques. Renewable and Sustainable Energy Reviews 2012;16(4):1926-1939. DOI: 10.1016/j.rser.2011.12.004

[13] Paraschivoiu I, Wind Turbine Design with Emphasis on Darrieus Concept. Polytechnic International Press, Canada; 2002.

[14] Simão Ferreira CJ, van Bussel G, van Kuik G. An analytical method to predict the variation in performance of a H-Darrieus in skewed flow and its experimental validation. Proc. of the European Wind Energy Conference, February 27-March 2, 2006, Athens (Greece); 2006.

[15] Bianchini A, Ferrara G, Ferrari L, Magnani S, An improved model for the performance estimation of an H-Darrieus wind turbine in skewed flow. Wind Engineering 2012;36(6):667-686. DOI: 10.1260/0309-524X.36.6.667

[16] Balduzzi F, Bianchini A, Maleci R, Ferrara G, Ferrari L. Blade design criteria to compensate the flow curvature effects in H-Darrieus wind turbines. Journal of Turbomachinery 2015;137(1):1-10. DOI: 10.1115/1.4028245

[17] Migliore PG, Wolfe WP, Fanucci JB, Flow curvature effects on Darrieus turbine blade aerodynamics. Journal of Energy 1980;4(2):49-55. DOI: 10.2514/3.62459

[18] Bianchini A, Balduzzi F, Rainbird J, Peiro J, Graham JMR, Ferrara G, Ferrari L, On the Influence of Virtual Camber Effect on Airfoil Polars for Use in Simulations of Darrieus Wind Turbines. Energy Conversion and Management;106(December 2015):373-384. doi:10.1016/j.enconman.2015.09.053.

[19] Bianchini A, Balduzzi F, Ferrara G, Ferrari L, A computational procedure to define the angle of attack on airfoils rotating around an axis orthogonal to flow direction. Paper submitted for publication to Journal of Turbomachinery.

[20] Hua Yang, Wenzhong Shen, Haoran Xu, Zedong Hong, Chao Liu, Prediction of the wind turbine performance by using BEM with airfoil data extracted from CFD, Renewable Energy, Volume 70, October 2014, Pages 107-115, ISSN 0960-1481, http://dx.doi.org/10.1016/j.renene.2014.05.002.

[21] Young-Tae Lee, Hee-Chang Lim, Numerical study of the aerodynamic performance of a 500 W Darrieus-type vertical-axis wind turbine, Renewable Energy, Volume 83, November 2015, Pages 407-415, ISSN 0960-1481, http://dx.doi.org/10.1016/j.renene.2015.04.043

[22] Balduzzi F, Bianchini A, Maleci R, Ferrara G, Ferrari L, Critical issues in the CFD simulation of Darrieus wind turbines. Renewable Energy 2016;85:419-435. DOI: 10.1016/j.renene.2015.06.048

[23] Balduzzi F, Bianchini A, Gigante FA, Ferrara G, Campobasso MS, Ferrari L, Parametric and Comparative Assessment of Navier-Stokes CFD Methodologies for Darrieus Wind Turbine Performance Analysis. Proc. of the ASME Turbo Expo 2015, Montreal, Canada, June 15-19, 2015. DOI: 10.1115/GT2015-42663

[24] Ansys, Inc., 2013, Fluent Theory Guide, release 14.5. 4.

[25] László Daróczy, Gábor Janiga, Klaus Petrasch, Michael Webner, Dominique Thévenin, Comparative analysis of turbulence models for the aerodynamic simulation of H-Darrieus rotors, Energy, Available online 24 August 2015, ISSN 0360-5442, http://dx.doi.org/10.1016/j.energy.2015.07.102.

[26] Maître T, Amet E, Pellone C, Modeling of the Flow in a Darrieus Water Turbine: Wall Grid Refinement Analysis and Comparison with Experiments. Renewable Energy 2013;51:497–512. DOI: 10.1016/j.renene.2012.09.030

[27] Raciti Castelli M, Englaro A, Benini E, The Darrieus Wind Turbine: Proposal for a New Performance Prediction Model Based on CFD. Energy 2011;36(8):4919–4934. DOI: 10.1016/j.energy.2011.05.036

[28] Bianchini, A., Balduzzi, F., Rainbird, J., Peiro, J., Graham, J M.R., Ferrara, G. and Ferrari, L., 2015, "An Experimental and Numerical Assessment of Airfoil Polars for Use in Darrieus Wind Turbines. Part 2 - Post-Stall Data Extrapolation Methods," Journal of Engineering for Gas Turbines and Power 2016;138(3). DOI: 10.1115/1.4031270

[29] Menter FR, Two-Equation Eddy-Viscosity Turbulence Models for Engineering Applications. AIAA J. 1994:32(8):1598–1605.

[30] Langtry RB, Menter FR, Correlation-based transition modeling for unstructured parallelized computational fluid dynamics codes. AIAA Journal 2009:47(12):2894–2906.

[31] Lanzafame R, Mauro S, Messina M, 2D CFD modeling of H-Darrieus wind turbines using a transition turbulence model. Energy Procedia 2014;45:131-140.

[32] Bianchini A, Balduzzi F, Rainbird J, Peiro J, Graham JMR, Ferrara G, Ferrari L, An Experimental and Numerical Assessment of Airfoil Polars for Use in Darrieus Wind Turbines. Part 1 - Flow Curvature Effects. Journal of Engineering for Gas Turbines and Power 2016;138(3). DOI: 10.1115/1.4031269.

[33] Guntur S, Sørensen NN, Evaluation of several methods of determining the angle of attack on wind turbine blades. Proc. of The science of Making Torque from Wind 2012, Oldenburg, Germany, 09-11 October 2012.

[34] XFoil User Guide, available online at: http://web.mit.edu/drela/Public/web/xfoil, last access 02/10/2014

[35] Bianchini A, Ferrara G, Ferrari L, Pitch Optimization in Small-size Darrieus Wind Turbines, paper accepted for publication in Energy Procedia 2015.
[36] Vermeulen P, Builtjes P, Dejjer J, Bueren G, An experimental study of the wake behind a full-scale vertical-axis wind turbine. TNO Report 79-06118, 1979.
[37] Bianchini A, Ferrari L, Magnani S, Start-up behavior of a three-bladed H-Darrieus VAWT: experimental and numerical analysis. Proc. of the ASME Turbo Expo 2011, Vancouver (Canada), June 6-10; 2011. DOI: 10.1115/GT2011-45882